Stan ZUREK

Megger Instruments Ltd, Archcliffe Road, Dover, CT17 9EN, Kent, United Kingdom

doi:10.15199/48.2018.03.02

Systematic measurement errors of local B-coils due to holes

Abstract. *B-coils (search coils) for measurement of local value of flux density B are made by drilling holes in the sample under test. The holes are non-magnetic discontinuities and distort the B distribution. The FEM analysis and experimental results presented in this paper show that in the first approximation the measurement errors are proportional to the ratio of hole diameter to coil width. For example, for a 10 mm wide B-coil made with 1 mm holes the error can be around 10%. Hence, in order to achieve errors less than 1% the hole diameter should be less than 1% of the coil width.*

Streszczenie. *Cewki do pomiaru lokalnej wartości indukcji magnetycznej B są wykonane przez wiercenie otworów w testowanej próbce. Otwory te reprezentują niemagnetyczne nieciągłości i powodują zniekształcenie dystrybucji B. Wyniki analizy FEM i pomiarów zaprezentowane w artykuly wykazują że w pierwszym przybliżeniu błędy pomiarowe są proporcjonalne do stosunku średnicy otworów do szerokości cewki. Np. dla cewki o szerokości 10 mm i otworach 1 mm błąd może być ok. 10%. Dlatego też, aby uzyskać błąd mniejszy niż 1% to średnica otworu powinna być mniejsza niż 1% szerokości cewki pomiarowej B. (**Systematyczne błędy pomiarowe lokalnych cewek B powodowane otworami)**.*

Keywords: B-coil, search coil, pick-up coil, electrical steel, measurement error, measurement uncertainty.
Słowa kluczowe: cewka pomiarowa B, blacha elektrotechniczna, błąd pomiaru, niepewność pomiaru.

1. Introduction

Magnetic properties of soft magnetic materials like electrical steels are measured with the help of induction coils (also referred to as B-coils or search coils [1-10]) which detect flux density *B* averaged over the active cross-section area of the coil (Fig. 1).

According to Faraday's law, voltage induced in the coil is proportional to the number of turns n of the coil, the active cross-section area *A*, and the rate of change of *B* with respect to time *t* but averaged over *A*. The information about time variation of spatially-averaged *B* is thus obtained by integration of the function:

(1) $V = n \cdot A \cdot dB/dt$ (V)

It should be noted if equation (1) is to define the *measured* voltage across a B-coil then there is no minus on the right-hand-side. This minus appears only for the induced electromotive force.

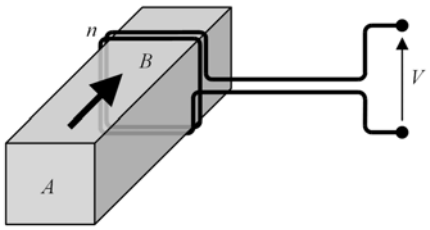

Fig.1. Concept of B-coil

Sometimes it is desirable to measure localised properties, which requires the use of the needle probes [1, 5, 8-10], or localised B-coils for which appropriate holes must be drilled in the sample under test [1-3, 5, 6-9]. The performance of needle probes can be severely affected by asymmetrical magnetisation [1, 9]. This can lead to indication of non-physical values of *B*, even significantly larger than the saturation of the material; results up to 4 T were reported in the literature [10].

B-coils are more immune to such problems and hence also used extensively for localised measurement [5]. However, the method is more destructive because holes must be drilled in the sample under test (Fig. 2).

The holes represent non-magnetic discontinuity and severely distort distribution of *B* in the immediate vicinity of holes. Qualitatively such effects are indeed well known and documented in the literature with both finite element modelling (FEM) [3] as well as surface scanning measurements [11]. However, from the viewpoint of uncertainty analysis these effects do not seem to be quantified sufficiently well in the literature. In some cases they are even completely neglected in the uncertainty analysis of the whole measurement system [5].

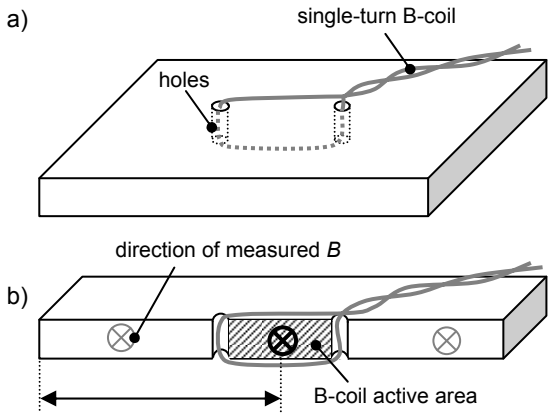

Fig.2. Local B-coil: a) overview, b) cross-section view with the arrow defining dimensions used in the following figures (drawings not to scale)

This article focuses on *quantitative* analysis of such errors for local B-coils. As evident from the results presented below there can be significant systematic measurement errors, which are far from negligible.

It should be stressed that the effects contribute to a systematic offset, not just an uncertainty. As it is shown below, this is because the discrepancy is always positive because the detected value is *always overestimated* and it depends on the appropriate dimensions of the given B-coil.

2. Distribution of B around holes

As soon as the holes are present the B distribution will be distorted around them. Such irregularities will be always present, to a smaller or larger degree due to the creation of local magnetic poles [4]. As a consequence, the local distribution is such that the magnitude of B tends to be very small at the part of the hole inner surface which is perpendicular to the direction of magnetisation, and it is elevated at the face which is parallel to it (Fig. 3 and Fig. 4).

This is a direct result of the circular shape of the hole, and the results agree with theory [4], 3D simulations [3] and experimental verification [11].

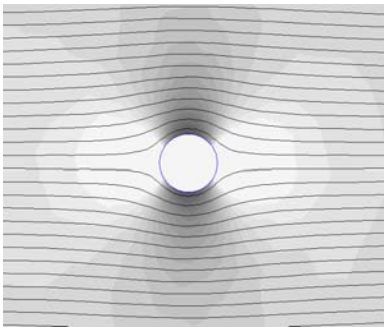

Fig.3. Typical distribution from 2D FEM of magnetic flux (lines) and *B* (grey scale); the grey scale map is from 0.9 T (white) to 1.5 T (dark grey)

The concentration of *B* extends some distance away from the hole so that if another hole is placed in the vicinity the elevated values "overlap" and will cause increase of averaged value of *B* over the active area of the coil.

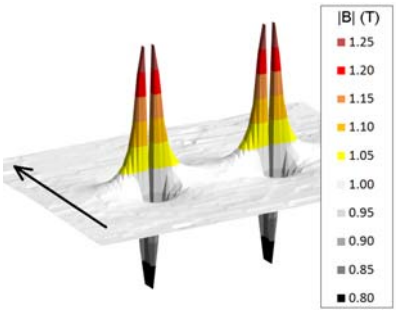

Fig.4. Distribution of modulus of B around a pair of holes from 3D FEM; the arrow shows direction of magnetisation

The local increase of *B* between the holes results in increased spatial average of *B*, which is therefore detected by the B-coil wound around such holes. This effect is often neglected if the holes are "small" so that an undeclared but implicit assumption is made that the disruption of the local distribution of *B* is unaffected and that any effects on *B* measurement errors are "negligible" and hence not taken into the measurement uncertainty budget [5].

Obviously, smaller holes introduce smaller disruptions. However, from practical viewpoint diameters smaller than 0.3 mm are very difficult to make and use, especially that at least one turn of wire has to be threaded through the holes. Hole diameters up to 0.8 mm and even greater are used in practice [1, 3, 5-7], and such values are larger than the thickness of lamination for typical electrical steels, which range between 0.18–0.5 mm.

For some measurements the typical B-coil width can be between 20–80 mm, with a pair or even multiple pairs of holes [1, 3, 5-7]. There arises a question of measurement errors or uncertainties which can be caused by using a given combination of hole diameter and B-coil width.

3. Simplistic analytical model

Let us assume a perfectly isotropic and linear ferromagnetic material such that its relative amplitude permeability μ_r is at least three orders of magnitude greater than unity, and that the material does not saturate. Under such assumptions in the first approximation any leakage effects can be neglected, because most flux will be concentrated in the highly permeable material, rather than in the surrounding air (including the air in the hole). For instance, with μ_r = 1000 the leakage directly through the hole would only constitute around 0.1% as compared to B in the material. Such small difference can be non-negligible, but as shown below much greater effects take place.

For simplicity, also the effects due to mechanical stresses induced during drilling are neglected. As it is shown below such assumption is correct.

When a cylindrical hole is drilled in a magnetic lamination the magnetic flux flows around it, similarly as illustrated in Fig. 5 (see also Fig. 3). As a result, in the immediate vicinity of the hole there will be some areas where the density of flux lines (i.e. flux density *B*) is increased and in some other areas will be reduced, as shown in Fig. 5. At a distance sufficiently far away from the hole the *B* distribution will be unaffected.

The assumed hypothetical magnetic material is linear, but with finite permeability. Therefore, some energy is stored in the magnetic field within the volume of the material (due to the $B \cdot H$ product). The displaced flux lines will not concentrate exactly at the edge of the hole, but will spread further away so that the energy is minimised.

In the very simplistic model shown in Fig. 5b just the flux lines which encounter the non-magnetic hole on their way are redirected. The drawing in Fig. 5a shows that there are four lines crossing the to-be hole, so that two lines will flow on one side of the hole, and two on the other side.

As a result, on each side of the hole, *B* would double for the width equivalent to the radius of the hole, whereas further from the hole it would be unaffected. Hence local *B* amplitude can reach 200% of the "uniform" value. Therefore, 0.1% of leakage will not significantly affect the overall picture, so it can be neglected in the first approximation.

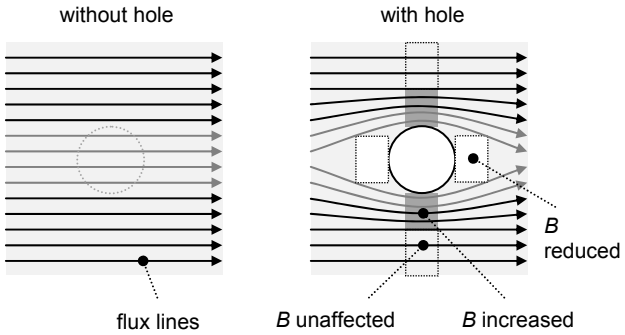

Fig.5. Simplistic linear isotropic model for a single hole

Such model does not take into account the actual energy distribution and the shape of "decay" of the increased *B* from the hole. However, even such simplistic approach illustrates the involved amplitudes and the mechanism behind elevation of *B* magnitude.

Local B-coil usually has a second hole close to the first one (Fig. 6). The presence of the two holes will introduce some elevated *B* between them.

The width *w* of the coil is assumed here as measured between edges of the holes (Fig. 6). The hole diameter is *h*, hence its radius is *h*/2. The "uniform" value of flux density is B_u (if the holes were not present).

Therefore, average *B* between the holes as detected by the B-coil (B_{coil}) will be a function of the dimensions so that:

$$B_{coil} = (B_u \cdot (w-h) + 2 \cdot B_u \cdot h) / w = B_u \cdot (1 + h / w) \quad \text{(T)} \tag{2}$$

If the presence of the holes could be neglected then it would be true that $B_{coil} = B_u$ but this is not the case in practice.

For a hypothetical B-coil with *w* = 10 mm and *h* = 1 mm it is easy to calculate from (2) that $B_{coil} = 1.1 \cdot B_u$ so the expected overestimation can be 10% of the "uniform" value. Such a large error is certainly *not* negligible.

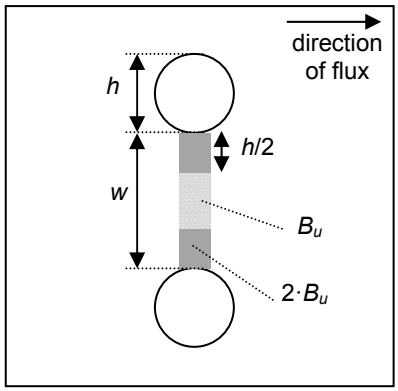

Fig.6. Simplistic linear isotropic model for 2 holes

4. FEM analysis with non-oriented electrical steel

FEM can be used for simulations which would include such effects as in-material energy storage and non-linearity due to magnetic saturation.

For this purpose FEM software was used: 2D package FEMM 4.2 [12] as well as 3D software COMSOL 5.2a [13] were employed. The FEM simulations were carried out only for magnetostatic case in order to fully take into account the non-linear magnetic behaviour of the material, rather than the quasi non-linear approximations used in the so-called time harmonics solvers [14, 15]. For the same reason, only isotropic properties were taken into account, and the investigation was focused on non-oriented electrical steel, grade M400-50 as pre-defined in the software [12, 13].

Typical results for 2D FEM are shown in Fig. 3, and for 3D FEM in Fig. 4. The agreement between 2D and 3D simulations was very good (Fig. 7). In the paper mostly results from 3D simulations are used.

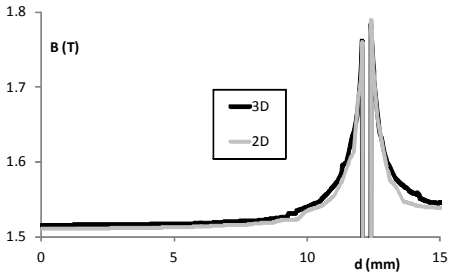

Fig.7. Typical agreement between 3D and 2D simulations by FEM

The sample under test was modelled as a single Epstein strip 30 x 300 mm (as normally used in the standardised Epstein frame method [14]).

The samples M400-50 (non-oriented electrical steel 0.5 mm thick) were measured in a non-standard single-strip yoke (Fig. 8a). The simplified version of the yoke (without the rounded corners) was used for 3D FEM (Fig. 8b).

Fig.8. Non-standard SST used for experiments (left) and its simplified version in 3D FEM calculations (right)

In FEM the excitation was varied from 0.1 T to 2 T. For this reason it was not possible to use actual B-H curves recorded from the samples, because sufficiently high excitation could not be applied with the experimental setup.

However, the used methodology should be acceptable for order-of-magnitude effects, because the samples were also made from M400-50. As shown below the agreement between simulated and experimental data is rather good, so such approach was justified.

The parameters of B-coils were varied by changing the diameter of the hole diameter *h* and the coil width *w*. Therefore, a characteristic parameter of the ratio *R* could be defined as:

(3) $R = h / w$ (unitless)

It can be concluded that the ratio *R* is proportional to the error resulting from equation (2).

A B-coil was assumed to be wound "tightly" around the active area (see Fig. 2) so that only the flux penetrating the active area was contributing. Such approach ensured that other effects (like leakage or air flux) would not significantly affect the total flux penetrating the simulated coil. As it is shown below even with such conservative approach the flux density is still always overestimated.

If the *B* distribution is non-uniform then the induced signal will be proportional to the value of *B* averaged over the area enclosed by the coil, regardless of the behaviour of the leakage flux outside of the coil. This paper focuses only on the effects caused by the non-uniform *B* distribution inside the material, with the assumption that otherwise the coil is "ideal".

In order to show the effect of the hole size, three B-coils were studied:

- C1 with w = 4.5 mm, h = 0.5 mm, R = 0.11 (≈ 0.1)
- C2 with w = 4 mm, h = 1 mm, R = 0.25 (≈ 0.2)
- C3 with w = 9 mm, h = 1 mm, R = 0.11 (≈ 0.1)

Typical results for 0.1 T excitation is shown Fig. 9. The *B* data is plotted through the width of the sample strip, from its edge to the centre. This is defined by the arrow in Fig. 2b. The value of distance d = 0 mm corresponds to the edge, and d = 15 mm is the centre of the strip.

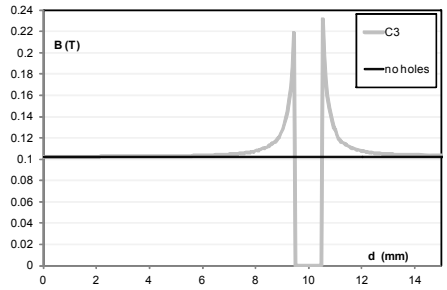

Fig.9. Typical FEM results at 0.1 T

As can be seen, the maximum value at the edge of the hole can indeed reach and even exceed 200% of the "uniform" value, as predicted by the simplistic model. At low excitation the material can be treated as almost linear, because permeability decreases significantly only above 0.5 T [15].

The amplitude "decays" with the distance from the hole, but also it can be seen that it extends over much greater distance than just the radius of the hole.

The "decay" of the increased *B* resembles exponential shape, which is probably dictated by the energy storage within material, as suggested above. However, the decay is modified at higher excitations by the *B-H* nonlinearity of the material.

As evident from Fig. 10, once the increased *B* is pushed to a level at which the permeability decreases it is more favourable for flux to spread wider (compare Fig. 9 and Fig. 10) so that the peak values are reduced below 200%.

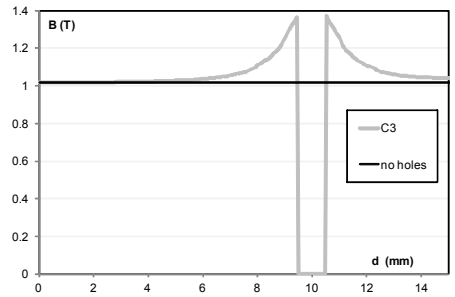

Fig.10. Typical FEM results at 1.0 T

For very high excitation of B_u = 2.0 T the flux spreads even wider (Fig. 11). The flux leakage through the hole is no longer negligibly small. However, the elevation of B around the holes is still pronounced and will still make B_{coil} to be elevated *significantly* above the B_u value. But it can be expected that the error would be smaller than for lower excitations.

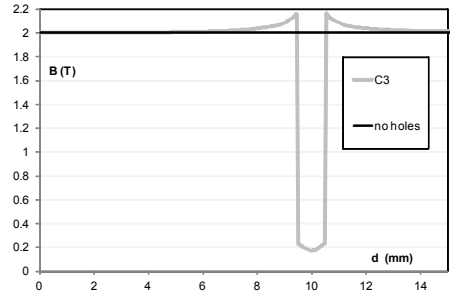

Fig.11. Typical FEM results at 2.0 T

Results in Fig. 12 show comparison for two B-coils of similar w, but different h, and by extension also different R. Clearly, the average of B between the holes is different, and non-negligibly higher than the value when the holes are absent.

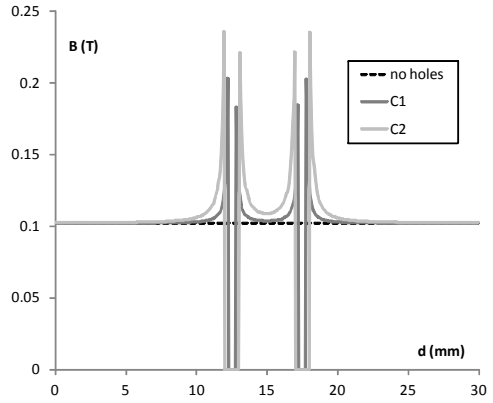

Fig.12. Typical results at 0.1 T across full width of the sample

It should be noted that in all cases the local increase in B is significant but the values reduce to the uniform value at sufficiently large distance from the hole (e.g. towards edges of the sample).

The maximum value around the hole does not significantly change with the hole size, and the shape of "decay" is almost the same for a given excitation level. This is illustrated in Fig. 13 which shows a comparison of 0.1 mm hole with 0.9 mm hole. When the 0.1 mm hole profile is scaled nine-fold the overall shape and amplitude matches very well that of the 0.9 mm hole. In this case 2D FEM was used because allowed application of much denser meshing so that resolution of the curve-plotting was improved.

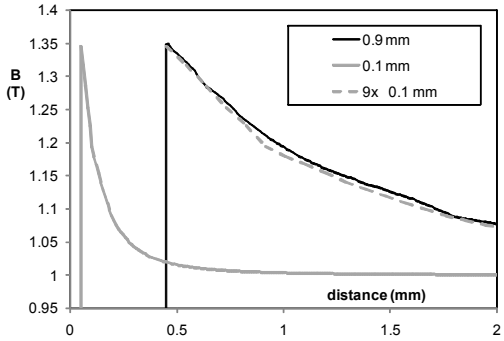

Fig.13. Shape of B distribution scales proportionally to hole size (2D FEM)

The spatial average can be calculated for a given coil and compared with the uniform value, so that the error can be estimated. Because the distribution changes with the level of excitation (Fig. 9, 10, 11) also the actual error level changes, rather than being fixed as calculated from the simplistic linear model.

The comparison between the results of FEM and those of simplistic model are shown in Fig. 14. The agreement is reasonably good, especially for lower excitations (1 T and below) where the material is not locally saturated.

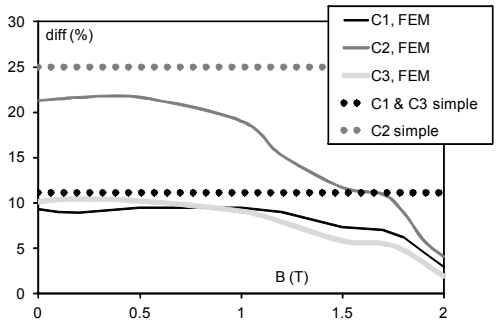

Fig.14. Comparison of results from FEM and the simplistic analytical model

However, even for higher excitations the systematic offset (error) could reach several percent. At 1.9 T the errors for coils C1, C2 and C3 are 4.6%, 5.8% and 3.4% respectively. At 2.0 T the values are 2.9%, 4.0% and 1.9% respectively.

Therefore, the simplistic model could offer a quick estimation of the likely maximum errors for local B-coils, especially at lower excitations.

5. Measurements on non-oriented electrical steel

As mentioned above, M400-50 non-oriented steel was used for the experimental verification. The magnetising yoke of a single-strip tester is shown in Fig. 8a. The results shown in this section are only for non-controlled waveshape of excitation. Further details are given below.

Holes were drilled in the sample strips as shown in Fig. 15. Their exact locations were measured with digital microscope Inspex HD1080p [16]. The measured values were averaged from three readings and rounded to the nearest 0.01 mm. The parameters of the experimental B-coils were as follows:

- C1, w = 5.12 mm, h = 0.43 mm, R = 0.084 (≈ 0.1)
- C2, w = 5.15 mm, h = 0.99 mm, R = 0.19 (≈ 0.2)
- C3, w = 9.96 mm, h = 0.98 mm, R = 0.098 (≈ 0.1)

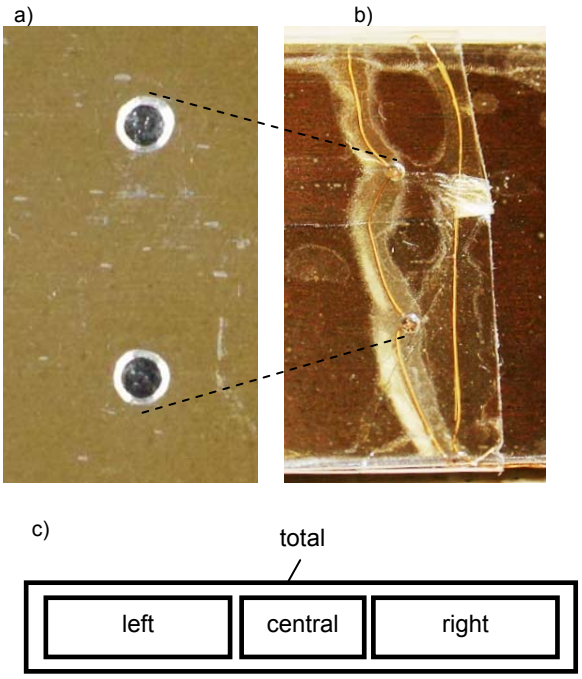

Fig. 15. Experimental coils: a) holes drilled in the sample, b) B-coils made with 0.1 mm enamelled wire, c) illustration of four B-coils placed at the same location

All three coils were made on the same sample, but spaced away by at least 50 mm from each other.

The intention was that the experimental B-coils were similar to those used in FEM simulations, so that the values of *R* are of similar order of magnitude, and *R* for C2 is roughly twice as large as for C1 and C3. Therefore, the expected errors should follow the same order-of-magnitude changes.

The samples were annealed in a controlled gas atmosphere after drilling so that the residual mechanical stresses were removed.

Each pair of holes allowed making four B-coils as illustrated in Fig. 15b and 15c. The investigation focused on calculating errors from the "central" coil with respect to the "total" coil, which encircled the whole sample.

As seen in Fig. 15b, the "total" coil was placed at some distance away from the pair of holes so that the local distortion in *B* distribution would not influence the measurement.

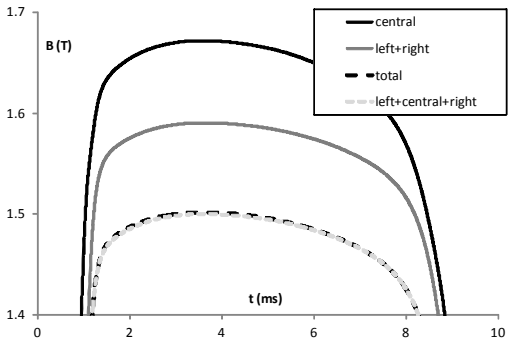

Fig. 16. Agreement of "total" and sum of voltages of "left+central+right" as well as elevated B in the "central" coil, 60 Hz, 1.5 T, coil C2

In the first approximation it can be assumed that the flux leakage through the holes can be neglected for low and medium excitations (Fig. 9 and Fig. 10). Therefore, the total flux enclosed by the "total" coil and the smaller coils should be the same and the sums of the voltages should be also equal. Indeed, the agreement was very good, not exceeding 1% and typically better than 0.5% not only at various excitation levels but also throughout the waveform on a point-by-point basis. A typical example for C2 measured at 1.5 T at 60 Hz is shown in Fig. 16. For clarity the curves show magnified part of just the positive half-cycle of measured *B* waveforms.

As can be seen from Fig. 16 the value of *B* measured with the "central" coil is significantly elevated over the uniform value (which is represented by the "total" coil).

It should be noted that also the "left+right" value is elevated, because *B* was also increased on the outside of the central B-coil – towards the edges of the sample (see also Fig. 12).

The same behaviour was measured under different excitation conditions. For example, as shown in Fig. 17 even at high excitation the elevation of *B* in the "central" coil is still significant and in this case reached the peak reached 2.06 T versus 1.89 T of the "total" coil. However, it is evident that the percentage differences remain very similar throughout the whole waveform.

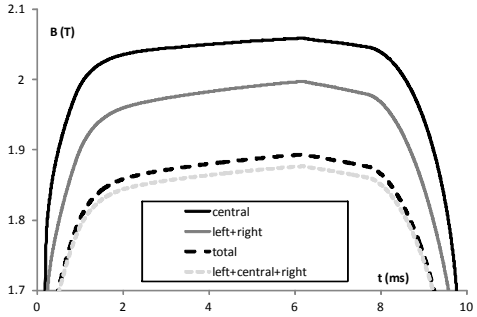

Fig. 17. Agreement of "total" and sum of voltages of "left+central+right" as well as elevated B in the "central" coil, 60 Hz, 1.9 T, coil C2

Indeed, the errors calculated from the measured waveforms agree very well with those simulated in FEM. The comparison of all the curves is shown in Fig. 18. It is clear that for lower excitation the B-coils with $R \approx 0.1$ (C1 and C3) produce errors of around 10% whereas the B-coil with $R \approx 0.2$ (C2) results with errors around twice as large.

It is not practical to drill holes smaller than 0.3 mm and use them for threading a wire without damaging its insulation. However, the behaviour can be studied with the help of FEM, because of good agreement between experiment and simulations (Fig. 18).

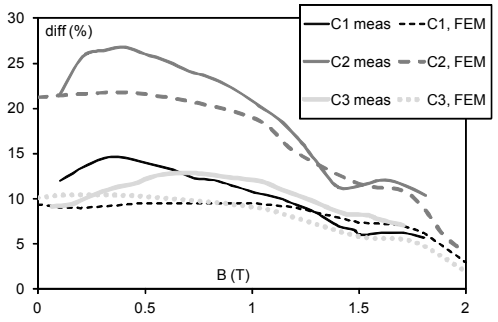

Fig. 18. Comparison between FEM and measurements (meas)

Simulations were carried out for a 10 mm wide B-coil. Under the same excitation the hole size was gradually

reduced from 2 mm to 0.01 mm, so that R changed from 0.2 (20%) to 0.01 (1%). The results are shown in Fig. 19.

In the first approximation the relationship is linear, especially for medium and low excitation. It is evident that in the worst case in order to achieve < 1% error it would be required to produce a B-coil with equivalent of R < 0.01.

This suggests that if the smallest practical hole diameter is 0.3 mm then the B-coil width should be at least w = 30 mm. However, if it is required to achieve < 0.1% error then the coil would have to be 300 mm wide.

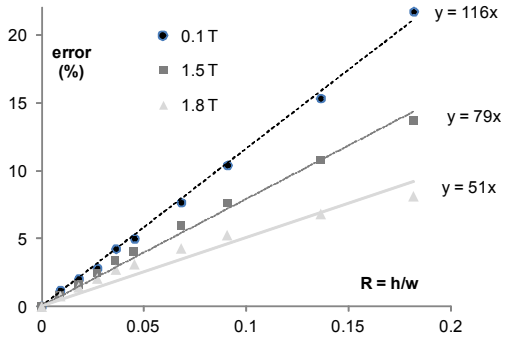

Fig. 19. B-coil errors vs. R and excitation level (3D FEM)

The data from Fig. 19 confirm some results quoted in the literature, even though the actual source of error was not defined previously. For instance, in [6] there are B-coils with w = 20 mm and h = 0.8 mm, which is equivalent to R = 0.04. Using the data from Fig. 19, depending on the excitation level the span of expected errors could be anywhere between 2.0% and 4.6%. The actual error stated in [6] was 2.7%, which is well within the range estimated from Fig. 18.

6. Other magnetising conditions

The results presented above were only for non-controlled waveshape of excitation because higher peak value of B could be applied under such conditions. However, very similar results were achieved under controlled sinusoidal flux density. The results are not shown here for brevity.

The same sample and coils (C1, C2 and C3) were used for measurements at 60 Hz and 1 kHz (Fig. 20).

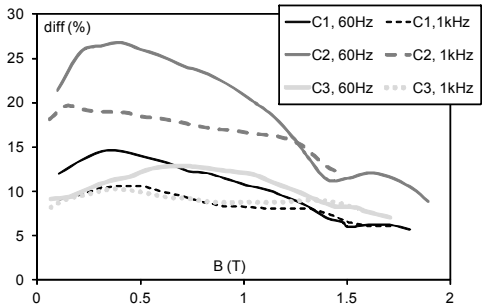

Fig.20. Comparison of experimental results at 60 Hz and 1 kHz

The curves follow similar shapes, with the same order of magnitude of errors, so that the C2 coil reads around double than the other two coils.

Therefore, these effects are maintained from DC conditions (FEM simulations) to at least 1 kHz, and the expected errors should be roughly the same.

7. Results for grain-oriented electrical steel

An experiment was also attempted with conventional grain-oriented electrical steel (typical grade M4). However, it is quite clear that the local anisotropy of the sample was capable of dictating the path of the flux to a much greater extent.

As evident from Fig. 21, for small and medium excitation (below the "knee" of B-H curve) the flux density detected in coil C2 was as much as 15% *lower* compared to the nominal value. On the other hand, coil C1 showed an increase exceeding 20% even though according to the simple model it should be only around +10%.

Therefore, in this particular case the size of the B-coils was too small in order to guarantee sufficient spatial averaging, so that the influence of the individual grains would average out.

However, it can be seen from Fig. 21 that at higher excitation the error for C2 does become the greatest similarly to the non-oriented steel presented above.

This occurs above 1.5 T which is above the "knee" of B-H curve. At such excitation the crystallographic energy of local crystallites begins to be overcome and the local B vectors are forced to align closer to the direction of the applied excitation.

As seen in Fig. 21, above 1.7 T the actual errors become such that C2 > C1 > C3 which corresponds to their ratios which were 0.19 > 0.098 > 0.084, respectively.

All the errors reduce at higher excitation, as they did also for the non-oriented steel, as shown in Fig. 18. At excitation above 1.7 T all the errors were definitely positive, with the smallest value +3.5% for the coils presented here.

Therefore, the systematic offset is also present in the grain-oriented material, it is just that the localised grain influence masks its behaviour so that it amplitude cannot be as easily detected as for the non-oriented steel.

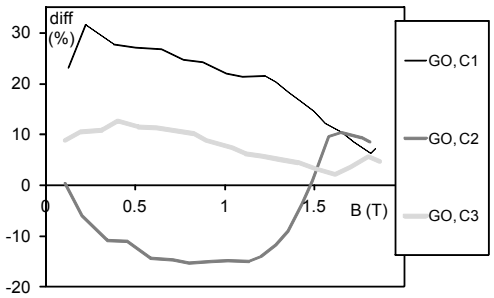

Fig.21. Results for conventional grain-oriented electrical steel measured at 60 Hz

Incidentally, the data in Fig. 21 reveals the great influence which local grain structure can have on the measurement of B. Local B-coils are used for example in rotational power loss measurement in which it is common to have poor repeatability of results from sample to sample [7]. In such measurements the B-coils can be as small as round 20 mm, so it is clear than in the worst case the effects can be quite significant (as per Fig. 18), with the flux directed away as well as into the active area of such B-coil. In both cases the B will be measured incorrectly, because the underlying offset will be always there, but there will also be the additional variability due to localised grains.

8. Comments on alternative approach

As an alternative approach the active width of the B-coil could be assumed between hole centres rather than from their edges.

But this would just scale the active area by a fixed value. If this is applied to the data for the non-oriented steel then the measured error curves would look like shown in Fig. 22.

The errors for the lower excitation are reduced somewhat, but the errors for the high excitation are exacerbated significantly but with a changed sign.

As a result the overall peak-peak error is still comparable directly to the ratio *R*. The systematic offset is reduced only for the intermediate values, but it remains significantly positive for the lower values, and significantly negative for high values.

Therefore, if the measurements are to be performed at higher excitation then assuming the hole edge to hole edge active area would always produce lower errors than the hole centre to hole centre approach.

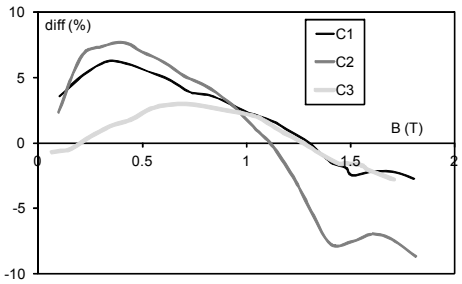

Fig. 22. Alternative approach for non-oriented steel, 60 Hz

9. Summary and conclusions

Holes drilled in the sample represent magnetic discontinuities which create flux crowding around the holes during magnetisation. As a result, the average *B* between the holes is greater than the uniform *B* at large distance away from the B-coil.

As a result the spatially averaged value of *B* detected by such B-coil is *always higher* than the ideal case without holes. The overestimation is directly proportional to the ratio $R = h / w$ of the hole diameter *h* to B-coil width *w*.

In some publications the width of local B-coil is given as around 20 mm. As shown in this paper, in order to achieve systematic error smaller than 1% it would be required for the holes to have diameter smaller than 0.2 mm ($R < 0.01$). Such holes are difficult to make. In practice 0.3 mm is more achievable, but this would require coil width of at least 30 mm in order to ensure that $R < 0.01$.

Obviously, if 0.1% error is to be achieved then the ratio would have to be $R < 0.001$, which for a practical hole size of 0.3 mm would require B-coil width of 300 mm.

Under any circumstances, the systematic errors due to the presence of the holes should not be dismissed as "negligible" because for dimensions used in practice they can amount to several percent.

If a local B-coil is used to control the level of *B* then the applied magnetisation will be lower than expected, because the detected signal will be higher than it should have been. Therefore, the accuracy of comparison between different apparatus using B-coils with different *R* parameter might be adversely affected even further.

The systematic errors of local B-coils arising from the distortions around the holes can be guaranteed to be kept below any level, provided that the coils were made with sufficiently small R parameter, as analysed in this paper.

Although the word "error" was used throughout the paper it is quite clear that the simple offset correction is not possible and that the level of difference can vary significantly. For this reason it is more appropriate to talk about uncertainty of flux density measurement as caused by the presence of the holes drilled in laminations.

The author would like to thank Dr Wojciech Pluta of Czestochowa University of Technology, Poland for supplying the samples and Mr Christopher Waller of Megger Instruments Ltd, UK for precision drilling.

The author is also indebted to Mr David Woolger of Magnetic Shields Ltd for providing specialised laboratory equipment and for annealing the samples under controlled conditions.

***Authors**: Dr Stan Zurek, Megger Instruments Ltd, Archcliffe Road, Dover, CT17 9EN, Kent, United Kingdom, Stan.Zurek@ieee.org*

REFERENCES

[1] Loisos G., Critical evaluation and limitations of localised flux density measurements in electrical steels, IEEE Trans. Magnetics, Vol. 37 (4), 2001, p. 2755

[2] Tumanski S., Induction coil sensors – a review, *Measurement Science and Technology*, Vol. 18 (3), 2007, p. R31

[3] Borg Bartolo J., et al., An investigation into the geometric parameters affecting field uniformity in four pole magnetisers, presented at *13th International Workshop on 1&2 Dimensional Measurement and Testing*, Turin, Italy, 2014

[4] Fiorillo F., Measurement and Characterization of Magnetic Materials, Elsevier Series in Electromagnetism, *Elsevier Academic Press*, 2004, ISBN 0-12-257251-3

[5] Sievert J., et al., Intercomparison of measurements of magnetic losses in electrical sheet steel under rotation flux conditions, *Commission of the European Communities, Report EUR 16255 EN*, EC Brussels, Luxembourg, 1995

[6] Gorican V., et al., Unreliable determination of vector B in 2-D SST, *Journal of Magnetism and Magnetic Materials*, Vol. 254-255 (2003), 2003, p. 130

[7] Zurek S., et al., Errors in the power loss measured in clockwise and anticlockwise rotational magnetisation. Part 2: Physical phenomena, *IEE Proceedings, Science, Measurement and Technology*, Vol. 153 (4), 2006, p. 152

[8] Loisos G., Novel Flux Density Measurement Methods of Examining the Influence of Cutting on Magnetic Properties of Electrical Steels, *PhD thesis, Wolfson Centre for Magnetics, Cardiff University*, Cardiff, UK, 2002

[9] Oledzki, J.S., Validation of the needle method for magnetic measurements, *Proceedings of 7th 1&2DM Workshop*, Braunschweig, PTB, 2003, p. 203

[10] Pfutzner H., et al., The needle method for induction tests: sources of error, IEEE Trans. Magnetics, Vol. 40 (3), 2004, p. 1610

[11] Tumanski S., Non-destructive testing of the stress effects in electrical steel by magnetovision method, *Non-linear electromagnetic systems, ISEM 99, IOS Press*, 2000, p. 273

[12] Meeker D., FEMM, Finite Element Method Magnetics, http://www.femm.info

[13] COMSOL Multiphysics, http://www.comsol.com

[14] IEC 60404-2, Methods of measurement of the magnetic properties of electrical steel strip and sheet by means of an Epstein frame

[15] Non Oriented, Fully Processed, Electrical Steel Catalogue, *COGENT*

[16] Ash Vision, Digital Microscope Inspection Systems, Inspex HD 1080p